FR 7900514

C.E.N. SACLAY
D.M.E.C.N.
DEPARTEMENT DE TECHNOLOGIE
Section de Recherches de Métallurgie Physique

Workshop on Solute Segregation and Phase Stability during Irradiation, Gatlinburg, Etats-Unis, 1-3 novembre 1978.
CEA-CONF-4482

RADIATION INDUCED HOMOGENEOUS PRECIPITATION IN UNDERSATURATED SOLID-SOLUTIONS

PRESENTATION A LA CONFERENCE :

WORKSHOP ON "SOLUTE SEGREGATION AND PHASE STABILITY DURING IRRADIATION"

GATLINBURG (TENNESSEE) U.S.A. - 1-3 NOVEMBRE 1978

PAR

RICHARD CAUVIN - C.T.T. - S.R.M.P.
GEORGES MARTIN - AGENT C.E.A. - S.R.M.P.

1e 19 Octobre 1978

WORKSHOP ON "SOLUTE SEGREGATION AND PHASE STABILITY DURING IRRADIATION"

GATLINBURG (TENNESSEE) U.S.A. - 1-3 NOVEMBRE 1978

RADIATION INDUCED HOMOGENEOUS PRECIPITATION IN UNDERSATURATED SOLID-SOLUTIONS

BY

RICHARD CAUVIN AND GEORGES MARTIN

Centre d'Etudes Nucléaires de Saclay
Section de Recherches de Métallurgie Physique
Boite Postale n°2 - 91190 GIF SUR YVETTE France

I - INTRODUCTION

It is now experimentally well established, that irradiation by energetic particles may not only accelerate solid state phase transformations, but also maintain solid solutions in (quasi-) steady-states which differ from the thermodynamical equilibrium state outside irradiation. Examples of such radiation *induced* (as opposed to accelerated) phase transformations are listed in a companion paper [1].

A well documented example is provided by radiation induced precipitation in Ni base *undersaturated* solid solutions. In Ni Si [2-4,7], Ni Ge [4,5,8], Ni Be [6] undersaturated solid solutions, radiation induced precipitation of respectively Ni_3 Si, Ni_3 Ge and β Ni Be has been observed under a wide variety of irradiation conditions. In the particular case of Ni Si and Ni Ge undersaturated solid solutions it has been proved that the condition for irradiation to trigger precipitation is that the *instantaneous irradiation flux* is larger than a composition-and temperature- dependant flux threshold, in complete agreement with an early suggestion by Adda *et al* [17].

The irradiation *flux* therefore appears to be an intensive control parameter of the state of solid solutions under irradiation and a tentative representation of the Ni rich side of the flux x temperature x composition phase diagram of Ni Si under irradiation could be proposed [9].

Most strikingly however, despite the fact that outside irradiation Ni Si supersaturated alloys provide a classical example for *homogeneous* second phase nucleation, the radiation induced precipitates in undersaturated solid solutions allways[*] appeared to decorate extended lattice defects, such as free surfaces, grain boundaries, dislocation lines, interstitial loops [2-4,7,11]. A similar behaviour was found in the Ni Ge [5] and Ni Be [6,10] systems. This observation favoured the interpretation of radiation induced precipitation in terms of non equilibrium solute segregation at point-defect sinks produced by the drag of solute atoms by the fluxes of point-defects towards these sinks [12-14]. Second phase precipitation is assumed to occur when the solute concentration at the point-defect sink becomes larger than the solute solubility limit outside irradiation. Such a mechanism indeed well accounts for the high temperature stability limit of the Ni Si solid solution [3,4,9].

The question therefore is raised to know whether this mechanism is the only one to operate ; if this is the case, radiation induced precipitation would allways be associated to point defect sinks, i.e. would allways be *heterogeneous*. Moreover, it can be proved [15] that the model, in it's present form [13,14] only predicts radiation induced *extension* of the two phase field of binary alloys, but not the reverse.

On the other hand, on purely theoretical grounds, Maydet and Russell[16] have argued that *homogeneous* nucleation may be triggered by irradiation in undersaturated solid solutions provided that the second phase embryo is *incoherent* and that the atomic volume of the precipitate is *larger* than that of the matrix.

To our knowledge, however this prediction has not yet received experimental confirmation.

---

[*] *In the particular case where radiation induced Ni_3 Si precipitates formed modulated structures, a one to one correspondance between precipitates and dislocation loops could not be established due to the difficulty if analysing the contrast of the very fine scaled structure which developed* [4].

In this context, we are exploring the stability of various types of solid solutions under irradiation. In this paper, we report observations made on Al Zn solid solutions under 1 MeV electron irradiation. Al Zn was chosen as a prototype of solid solutions with a simple miscibility gap. In §§ 2 we show that under appropriate irradiation conditions, *undersaturated* Al Zn solid solutions give rise to a *homogeneous* precipitation of *coherent* G.P. zones and (/or) of *incoherent* Zn precipitates the atomic volume of which is *smaller* than that of the matrix . As just recalled, none of the available theories accounts for such processes. In the 3rd§§ we propose a more general treatment of solute concentration heterogeneities in solid solutions under irradiation and suggest how it might account for the *nucleation* of the observed phases. The 4th §§ deals with the *growth* of the observed precipitates.

2 - THE BEHAVIOUR OF Al Zn DILUTE SOLID SOLUTIONS UNDER 1 MeV e^- IRRADIATION

2-1 *Experimental procedure*

Al 1.9 at % Zn alloy (with less than 300 wtpm overall purity) was kindly provided by P.U.K. company. For this Zn composition, the Zn incoherent solvus temperature is 110°C according to Hansen [18] and the coherent G.P zone solvus temperature is 45° according to the recent determination of Pelletier *et al.* [19]. At such a low zinc content, the α'_R phase has never been observed. It is worth noticing however that following a recent TEM study of the thermal decomposition of Al 6.8 at % Zn solid solutions, it was suggested that G.P zones and α'_R phase are simply early and late forms of a unique metastable coherent phase [20].

Samples in the form of 3 mm disks are punched from a 150 µm thick rolled sheet. These are solution annealed for one hour at 400°C in silica tube filled with argon. Rapid quenching to 150°C allows for the decrease of the vacancy concentration, therefore inhibiting the aging at room temperature. After one hour annealing at 150°C the samples are water quenched and then stored in liquid Nitrogen. Electron microscope specimens are prepared with a double jet electropolishing machine (Tenupol) using a 66 % methanol, 33 % nitric acid bath at -40°C.

The irradiations are performed in the 1 MeV HVEM of CNRS-ONERA[::]. Prior to irradiation, specimens are reannealed *in situ* in the hot stage of the electron microscop (half an hour at 235°C) and then brought directly to the irradiation temperature which ranged from 235°C to 95°C. As shown previously [3], the temperature increase under irradiation is less than 10°C with respect to the thermocouple reading. The 1 MeV electron flux ranged from 1.5 10^{20} to 5.10^{18} $e^- cm^2 s^{-1}$ as measured with a Faraday cup. The corresponding displacement rates range from 9 10^{-3} to 3 10^{-4} dpa s^{-1} using 16 eV for the average displacement threshold energy [21] and the displacemen. cross sections given by Ohen [22]. The irradiation conditions are given in more details in table I. Due to the lack of quantitative data [23] no correction was made for the orientation dependance of the displacement rate. The thickness of the irradiated zone is roughly 5000 Å. Detailed post irradisation observations are done with a Siemens Elmiscop 102 electron microscope operated at 125 kV.

2-2 *Typical radiation damage observed*

Radiation effects studies in Al Zn are rare [23-33] and deal all with supersaturated solid solutions. Low temperature (4.5 K or 78 K) deuteron [24] or neutron [25,26] irradiation is reported to have no effect on G.P zone formation in quenched supersaturated solid solutions, and to destroy the G.P. zones in aged alloys [27]. However, during post irradiation annealing, enhanced G.P zone formation is observed above 165°K which corresponds roughly to stage III of pure Aluminium. Vacancy mechanism is therefore thought to be the dominant diffusion mechanism of Zinc during G.P zone formation, although the contribution of a slowly migrating interstitial is suggested by Schüle [29,30]. The displacement cascades are shown to have no effect on G.P zone nucleation [26].

On the other hand, room temperature high energy electron irradiation is reported to induce the growth of vacancy loops in Al 6.5 at % Zn [31] or the condensation of small interstitial clusters close to the surfaces of Al 1 at% Zn foils [32] or the formation of large vacancy type Frank loops in Al 0.5 at % Zn [33].

[::] *Some irradiations were performed on the AEI-HVEM of the Max Planck Institut für Physik at Stuttgart. We thank Dr Urban for providing access to this microscope.*

Faced with these contradictory informations a carefull analysis of the type of radiation damage produced in our samples has been done.

First of all, no trace of defect -or solute- clustering was noticed outside the irradiated area. Moreover, in situ observations have shown that the objects observed in the irradiated zone do form in the course of irradiation and not during the subsequent cooling of the sample. Stereomicroscopy showed that these objects lay well inside the bulk of the sample and not at the surface of the foil.

In the irradiated area, three distinct types of objects could be identified :

- Dislocation loops with a typical size ranging from 5 to 100 nm. All the loops are *interstitial* as determinded by the inside outside contrast method [34]. They are perfect or Frank type depending on the irradiation temperature (cf.2.3)

- β phase precipitates (Zn) with a diameter ranging from 5 to 100 nm ; these are spherical when small or plate like when they get larger. The β phase is identified by the diffraction spots of the HCP structure which may be unambiguously distinguished from those of the FCC matrix when a low index HCP plane coincides with a high index FCC plan (e.g. $(77\bar{2})_{FCC}$ // $(11\bar{2}\bar{1})_{HCP}$). The β phase has epitaxial orientation relationship with the FCC Aluminium matrix (e.g. (111) // (0001) and $[1\bar{1}0]$ // $[1\bar{1}00]$). A weak deformation contrast is sometimes visible around these precipitates (fig.1, a-c).

- Small clusters with a typical size 2 to 5 nm and an extremely high number density ($\simeq 3\ 10^{16}\ cm^{-3}$), which we identified as G.P. zones for the following reasons : under two beam dynamical conditions, they are difficult to observe. No black white deformation contrast is appearent (fig.2a). However, when these clusters grow,a weak deformation contrast appears. Under out of contrast conditions, the clusters are seen as weak black dots, therefore exhibiting a phase and (or) absorption contrast typical of a chemical heterogeneity [35]. Moreover, much in the same way as the G.P. zones observed after the decomposition of supersaturated Al Zn solid solutions, these clusters produce an intense hallo around the diffraction spots of the matrix and are well imaged under symmetrical multibeam conditions [36,37] (fig.2 b-d).

These clusters never grow very large and disappear when the β phase develops (fig.3). On the only basis of the above TEM contrast arguments, one cannot exclude the possibility that these clusters are small cavities, although it is difficult to see why a small cavity would exhibit no deformation contrast, while a larger one would do so. On the contrary, this is a well known feature of the G.P. zones in Al Zn [20]. A quantitative analysis of the phase contrast of these clusters should help to make a direct decision. Due to the prohibitive thickness of the irradiated zone, such an analysis has not yet succeeded.

Other objects have been observed much more scarcely and with much smaller a density : e.g. small tetrahedra or surface Zn precipitates. Their presence does not affect the overall behavior which we discribe below.

2.3 *Irradiation conditions for the occurence of the various damage structures*

Depending on the irradiation temperature and instantaneous flux, the following damage was observed (cf Table I and fig.4) :

Domain A : at low temperature, 95°C < T < 135°C, interstitial loops nucleate within the first minute of irradiation, grow with a broad distribution of sizes and finaly form a dislocation network. When they are resolvable, these loops are perfect. Loop nucleation is very sensitive to the precise orientation of the specimen ; at low flux it is confined along the extinction contours on the side of negative deviation,s,from the exact Bragg orientation. After an incubation time which depends on the irradiation temperature and flux, (the incubation dose is some dpa) G.P.zones appear uniformaly throughout the irradiated area with no spatial correlation with the dislocation loops. After still a longer time (incubation dose of the order of 10 dpa), the β precipitates appear and grow while G.P.zones disappear quickly (Fig. 3). Again there is no spatial correlation between the Zn precipitates and the dislocation loops.

At 95°C the β precipitates appear under high flux irradiation only. But since the incubation time for their formation is very large, it is not possible to conclude, without irradiating for prohibitively long period of time whether β phase would form or not under low flux irradiation.

It is worth recalling that domain A covers a temperature range which lays well above the coherent - and includes the incoherent - solvus temperature. No marked change of behaviour is noticeable accross this latter temperature.

Domain B : at intermediate temperatures ($150°C < T < T^{::}$)

From the first minutes of irradiation, small points appear and develop either into resolvable dislocation loops or into β phase precipitates. The loops are of Frank type, they grow slowly, with a much smaller density that the perfect loops observed in domain A, and a uniform size. When they are large enough they unfault and slip out of the foil thus preventing the formation of a dislocation network. The β precipitates nucleate with a density (roughly 4 10^{15} cm^{-3}) much larger than that of the loops. This trend reverts when reaching the threshold temperature $T^{::}$. After prolonged irradiation (some dpa) the size of the Zn precipitates saturates and is rather uniform. The limiting size decreases with increasing temperature. No G.P.zone could be observed.

Domain C : at higher temperature ($T > T^{::}$), only Frank loops do appear in much the same way as in domain B. Neither β precipitates nore G.P zones are visible. At still higher temperature, no Frank loop ever forms.

As shown by fig.4 and Table II, the temperature threshold $T^{::}$ ($\simeq 200°$) which separates the above domains B and C is flux dependant (30°C upwards shift for and order of magnitude increase of the flux). Indeed when Zn precipitation is not detected at low flux, while it is at high flux for the same temperature, the total irradiation dose used at lower flux is at least twice the incubation dose at high flux. We therefore conclude that Zn precipitation in undersaturated Al Zn solid solutions may occur under irradiatio provided that the irradiation flux is greater than a *temperature dependant flux threshold.*

Whe have checked by in situ post irradiation annealing experiments that all the clusters formed dissolve at a temperature which is smaller than the irradiation temperature. The minimum temperature for such a dissolution to be observable within a reasonnable time is 135°C.

As a summary, under the irradiation conditions which we have described, the coherent and incoherent solvus temperatures of Zn in Al 1.9 at % Zn are increased by roughly 100°C. A dose rate dependance of the incoherent solvus temperature could be established. Both *coherent* GP zones and *incoherent* β phase nucleation are homogeneous. As explained in paragraph 1 these observations cannot be accounted for by the available theories of radiation induced precipitation. In the following we briefly describe a new theoretical approach to second phase nucleation and extend the growth model proposed by Maydet and Russell [16] in a way which qualitatively accounts for the above observations.

3 - THEORETICAL APPROACH TO SECOND PHASE NUCLEATION UNDER IRRADIATION

For reasons explained in the companion paper [1], we do not think that the large shift of the solvus temperature which we have observed can be accounted for by the contribution of the radiation induced point defect supersaturation to the free energy of the solid solution. In other words, the precipitates which we observe cannot result from the growth of solute concentration fluctuations in an assembly of solvant atoms, solute atoms and *conservative* point-defects [**]. We therefore look for solute concentration fluctuations under irradiation which have their origin in the non conservative nature of the radiation produced Frenkel pairs. The drag of solute atoms towards (or away from) the point-defect sinks induced by the flux of point defects towards these sinks [12-14] is one such mechanism. It is however not general enough since we observed that no correlation exists between the location of the point defect sinks and that of the precipitates. We show in this paragraph that under irradiation, a coupling exists between point-defect fluxes and solute concentration heterogeneities, even in the absence of point defect sinks or point-defect precipitation. Radiation enhanced solute concentration fluctuations may result from this coupling.

3-1 *Point defect fluxes in the absence of point defect sinks or point defect condensation*

Due to the non conservative nature of Frenkel pairs, it is possible to maintain point defect fluxes under irradiation simply by applying an external field to the point defects. We shall be more specific about the origin of this field in section 3.2.

[**] *As discussed in* [1] *the basic assumption of a constrained thermodynamical equilibrium approach to phase stability under irradiation is that the point defect mutual recombination or elimination on fixed sinks has no other effect than maintaining the point-defect supersaturation at a steady state value.*

Indeed, when Frenkel pairs are uniformaly produced in a non uniform potential well, the point defects are drifted towards the bottom of their respective potential well, (Fig. 5), where they would accumulate in the absence of interstitial-vacancy mutual recombination. The annihilation reaction however, prevents the vacancy and interstitial concentration to reach their *thermal-equilibrium* profiles (i.e. with zero defect flux) : *steady state* profiles (non zero defect flux) may however be reached.

More precisely, consider an infinite medium where vacancies (v) and interstitials (i) are created at a uniform constant rate G, annihilate by mutual recombination with rate $K\, C_i\, C_v$ and diffuse in potential wells (U_v for vacancies, U_i for interstitials) with diffusion coefficients respectively equal to D_v and D_i. The flux of interstitials is given by :

$$\vec{J}_i = - D_i \left[\vec{\nabla} C_i + \frac{C_i}{k_B T} \vec{\nabla} U_i \right] \qquad (1)$$

with $k_B T$ for the Boltzman energy. A similar expression holds for the vacancy flux.

The balance equations for interstitials and vacancies are respectively [*]:

$$\begin{aligned} \frac{\partial C_i}{\partial t} &= G - K\, C_i\, C_v - \vec{\nabla} \cdot \vec{J}_i \\ \frac{\partial C_v}{\partial t} &= G - K\, C_i\, C_v - \vec{\nabla} \cdot \vec{J}_v \end{aligned} \qquad (2)$$

Therefore at steady state :

$$\vec{\nabla} \cdot (\vec{J}_i - \vec{J}_v) = 0 \qquad (3)$$

To be more specific, let us deal with one dimensional equations (planar geometry or spherical symmetry) and zero flux at the surface of the computationnal cell. Eq. 3, together with the above condition leads to :

$$\vec{J}_i(r) = \vec{J}_v(r) \qquad (4)$$

---

[*] *We assume in eq. 2 that the expression for the rate of mutual recombination is not affected by the existence of a non uniform potential. This approximation should hold if the range of the potential well is large compared to the point defect mean free path.*

According to (1), the condition for $\vec{J}_i$ or $\vec{J}_v$ to vanish everywhere, is :

$$C_i = C_i^o \exp - U_i / k_B T$$
$$C_v = C_v^o \exp - U_v / k_B T \qquad (5)$$

According to (2), the condition for such profiles to be steady state is :

$$0 = G - K C_i^o C_v^o \exp - \frac{U_i + U_v}{k_B T} \qquad (6)$$

Since G and K are constants and U_i and U_v are functions of the position, the condition (6) can be realized only if

$$U_i(\vec{r}) + U_v(\vec{r}) = \text{constant} \qquad (7)$$

Condition (7) is very restrictive indeed and is *not* expected to be fulfilled e.g. for elastic interactions.

Fig. 5 shows preliminary results of a numerical calculation of the fluxes predicted in a cell with spherical symmetry[::]. The values of the parameters used are given in the figure caption; they were chosen for the sake of computational simplicity. They do not pretend to represent any real system. The potential well for the interstitial has a sinusoïdal shape and is attractive towards the center of the cell. No potential acts on the vacancies. As can be seen, the steady state point defect fluxes (which are equal as expected) are directed towards the center of the cell, where the interstitials are being attracted. The divergence of the defect flux is negative at the center of the cell : as shown by eq. (2), this behavior shows that the defect mutual recombination overcompensates the defect production at the center of the cell, in agreement with the qualitative physical argument given at the beginning of section 3.1. A more detailed quantitative evaluation is under progress.

[::] *Several calculations of point-defect fluxes in the presence of an interaction force field with spherical coordinates have already been published* [38-42]. *None of these included the mutual recombination of vacancies and interstitials, so that the effect under discussion has been overlooked.*

3-2 *Application to solute concentration fluctuations under irradiation*

Due to the long range part of the interaction between solute atoms and point defects, each solute concentration profile produces a potential well for the point defects, which according to the above argument gives rise to a point defect flux. Owing to the coupling between the point-defect - and solute fluxes, the former will induce the latter which depending on its direction may amplify or decrease the solute concentration heterogeneity by which it was triggered. Table III summarizes the possible situations. As can be seen, an attractive interaction between solute and defects, together with a positive coupling between the defect and solute fluxes leads to an amplification of solute concentration heterogeneities. Second phase homogeneous nucleation might result as an extreme case of such an amplification; it is worth noticing that the two above conditions are fulfilled by Zn in Al [43, 44].G.P.zone re-solution might be expected in the reverse case. Al-Ge corresponds to such a case [43]. Experiments are underway to check this point.

Moreover, as shown by Fig. 5, $D_iC_i - D_vC_v$ is non zero at the bottom of the potential well, i.e. at an extremum of the solute concentration profile. Depending on the amplitude and sign of this quantity, point-defects will or will not agglomerate [45], and if they do so, the resulting cluster will be of interstitial or vacancy type. The proposed mechanism can therefore, in principle, account for the observed large variety of behaviours such as, radiation induced homogeneous precipitation, with coherent interface (i.e. without simultaneous defect precipitation) or with incoherent interface (i.e. with simultaneous defect consumption [16]), but also such as emission of interstitial loops from fixed climb source [46].

A more detailed mean field description of the above arguments is under progress.

In the next paragraph, we discuss the stability and growth under irradiation of the precipitates once they are formed.

4 - GROWTH AND STABILITY OF PRECIPITATES UNDER IRRADIATION

As far as *coherent* precipitates are concerned, according to the argument of section 3.2, we suggest that they will reach a steady state size and number density corresponding to the solute concentration profile in equilibrium with the point defect fluxes which it produces. We cannot guaranty

the unicity of this steady state nore it's stability without a more detailed formulation of the problem. Work in progress.

On the other hand the stability of *incoherent* precipitates may be studied by a quite general method proposed by Maydet and Russell [16]. We show in this section that releasing restrictive conditions assumed by these authors, allows for a qualitative explanation for the growth of the incoherent zinc precipitates and for their tendancy to reach a steady state size under irradiation.

4-1 *Summary of Russell's approach [16, 47]*

Radiation induced precipitation may be vizualised as a special case of point defect clustering. Predicting the occurence of precipitation under irradiation reduces to the description of the trajectories of clusters in a solute content - defect content space. With the reasonable assumption that vacancy and interstitials cannot coexist inside a solute cluster, the cluster space is a two dimensional one (Fig. 6) : the coordinate axis are the number of solute atoms x, and the net number of defects [*] n, in the cluster.

Depending on the relative magnitude of the arrival and emission rates of point defects and solute atoms at the clusters, these clusters will achieve different morphologies e.g. voids, solute plated voids, incoherent or coherent precipitates, interstitial loops decorated with precipitates etc... (Fig. 6).

As shown by Russell *et al.* [16, 47] the trajectories of the clusters in the (x, n) plane may be predicted provided that the free energy change associated with the cluster formation is known,as well as expressions for the rate of vacancies, interstitials and solute atoms impingement on the cluster. Up to now, this formalism has been applied to void nucleation [47] and incoherent precipitation under irradiation [16]. In this latter case, the theory accounts qualitatively for the observed radiation *accelerated* precipitation of the oversized solute Ge and Cu respectively in AlGe [48] and AlCu [49] *supersaturated* solid solutions, and predicts radiation induced growth of incoherent precipitates of *oversized* solute atoms in *undersaturated* solid solutions. The original publication [16] predicts no similar behavior for *undersized* solute atoms. In the next section we show this conclusion is not correct.

---

[*] *n is the difference between the number of solvant atoms which were removed from and of solute atoms which were brought to the precipitate. When n is positive the net number of vacancies which have been absorbed by the cluster is larger than the corresponding number of interstitials. n is the difference between these two numbers*

4-2 *Reanalysis of Russell's model*

We keep the basic ingredients of Russell's model, i.e. the expression for the free energy change on forming the precipitate particle (eq. 8 ref. 16) and the expressions for the various impingement rates (eq. 25-28 ref. 16). Following the procedure developed in ref. [16, 47] the velocity field of the clusters in the (n, x) plane may be constructed at least qualitatively if one knows the direction of the velocity in one point of this plane and the location of the nodal lines, i.e. the lines where one component of the velocity changes sign. The equations for these nodal lines are [::] :

$$n = x \left\{\delta + \frac{1}{2B} \ln \left[S_v \left(1 - \frac{\beta_i}{\beta_v}\right)\right]\right\} \qquad (8\ a)$$

$$n^2 = x^2 \delta^2 \left\{1 + \frac{2A}{3B \delta^2 x^{1/3}} - \frac{1}{B\delta^2} \ln S_x\right\} \qquad (8\ b)$$

where δ is the atomic volume misfit between the precipitate and the matrix ($\delta = (\Omega_p - \Omega_m) / \Omega_m$), A and B are thermodynamical parameters defined in ref. 16, S_v is the ratio of the actual to the equilibrium vacancy concentrations, S_x is the ratio of the actual to the saturation solute concentrations and β_i and β_v respectively the interstitial and vacancy impingement rates at the cluster. The nodal lines defined by eq. 8 a and 8 b intersect at two critical points : the origin and a second point which may or may not lay in the region of physical interest ($x > 0$). The direction of the cluster velocity in particular points of the (n, x) plane may be determined by simple inspection of the analytical form of the former (eq. 9-14 ref. 16). One finds that :

$$\frac{dx}{dt} < 0 \quad \text{at } n = 0 \qquad (9\ a)$$

$$\frac{dn}{dt} < 0 \text{ for } x \to 0^+ \text{ and } n > 0 \qquad (9\ b)$$

Conditions 9 a and 9 b together with eq. 8 a and 8 b allow for the construction of the directions of the clusters velocity in each part of the (n, x) plane of physical interest ($x > 0$).

As shown by fig. 6, the trivial critical point at the origin ($n = x = 0$) is a stable fixed point for the clusters, i.e. all clusters in the vicinity of the origin will disolve. The non trivial critical point, when it lays in the region $x > 0$, is a saddle point, therefore allowing for the growth of clusters.

[::] *In ref. 16, eq. 8 b is replaced by its positive square root (eq. 32 ref. 16). The negative root has been droped for unspecified reasons.*

In other words, *a necessary condition for precipitates to develop under irradiation is that the non trivial critical point defined by 8 a, 8 b has a positive x coordinate.* Solving 8 a and 8 b one finds for the coordinate of the critical point :

$$x^{*-1/3} = \frac{1.5}{A} \{\ln S_x + S_v \delta + \frac{1}{4B} S_v^2\} \qquad (10\ a)$$

$$n^* = x^* (\delta + \frac{S_v}{2B}) \qquad (10\ b)$$

where S_v is an effective vacancy supersaturation defined by

$$S_v = \ln [S_v (1 - \frac{\beta_i}{\beta_v})] \qquad (11)$$

The general behavior of x^* may be found by the graphical construction shown on fig. 7. Simple inspection of eq. 10a shows that $(x^*)^{-1/3}$ is proportional to the algebric measure of MM' on fig. 7.

As can be seen, positive values of x^* are predicted in four cases (Fig. 7)

a) $\delta > 0$ (oversized precipitate atomic volume) with
   a1 :either medium positive effective vacancy supersaturation ($S_v > S_{v1}^+$). This is the case originaly predicted by Maydet and Russell [16].
   a2 :or strongly negative S_v ($S_v < S_{v2}^+$). This condition may be achieved when $\beta_i/\beta_v \to 1$.

b) $\delta < 0$ with b1 :either medium negative S_v ($S_v < S_{v2}^-$)
   b2 :or large positive S_v ($S_v > S_{v1}^-$)

Therefore, the original model of Maydet and Russell [16] does predict radiation induced incoherent precipitation (i.e. $x^* > 0$), in the case of undersized precipitate atomic volume. We cannot decide if the precipitation of the β phase reported in section 2 refers to the case b_1 or b_2 in the absence of a detailed evaluation of the defect populations during the precipitation process. Work is in progress.

4-3 *Saturation of the size of the precipitates*

In the above model, the fact that the non trivial critical point is a saddle point results from the functional form of the free energy change on forming a precipitate (eq. 8 ref. 16) and from the assumption that β_i/β_v does not depend on the cluster composition. However, as dicussed in [16], when growing under irradiation, the precipitate develops a strain field. This strain

field must biais the impingement rates of interstitials and vacancies : β_i/β_v is therefore a function of the departure (U) of the cluster composition from the zero strain field composition ($U = n - x\delta = 0$). It is simple to show [50] that if an appropriate U dependance of β_i/β_v is introduced in the above model, the non trivial critical point may change from a saddle point to a stable fixed point, i.e. a point which attracts the clusters in its vicinity. Therefore the above argument accounts qualitatively for the saturation of the size of the β phase precipitates under irradiation. It is worth mentioning that no dynamical resolution mechanism has been called for, to account for this saturation, contrary to the existing model of coarsening under irradiation [51-54].

5 - CONCLUSION

A systematic TEM study of 1 Mev electron irradiation damage in Al 1.9 at % Zn solid solution over a wide range of irradiation flux and temperature shows that Zn precipitates form, under irradiation, at temperatures well above the Zn solvus temperature outside irradiation. The corresponding upward shift of the Zn solvus temperature under irradiation is dose rate dependent, thus defining a (temperature dependent) dose rate threshold for the occurence of Zn precipitation in AlZn undersaturated solid solutions. This new example of radiation *induced* precipitation exhibits entirely new features as compared to the cases reported up to now :

- The second phase nucleation is homogeneous. No correlation exists between the location of the precipitates and that of the point defect sinks.

- The precipitation of incoherent β phase with atomic volume smaller than that of the matrix, and of clusters which we argue to be coherent G.P. zones both occurs.

- The size of the incoherent β precipitates saturates at large dose.

None of the available models of radiation *induced* precipitation accounts for this overall behavior.

A general mechanism for the coupling of solute concentration fluctuations with the irradiation flux is proposed which qualitatively accounts for the formation of coherent G.P. zones and for the nucleation of solute clusters with more complex structures.

A reanalysis and generalization of Maydet and Russell's model [16] for

the growth of incoherent precipitates shows that it may qualitatively account for the observed growth and saturation of the size of the β phase precipitates.

A more detailed quantitative analysis of these various processes is under progress.

Acknowledgements : The stimulating interest of Dr Adda, for this research, and many usefull remarks of Pr Guyot, Drs Bourret, Barbu and Bocquet, are gratefully acknowledged.

BIBLIOGRAPHY

1. J.L. BOCQUET and G. MARTIN - This issue
2. A. BARBU and A.J. ARDELL - Scripta Met. 9 (1975) 1233
3. A. BARBU and G. MARTIN - Scripta Met. 11 (1977) 771
4. A. BARBU - Thesis (Nancy, France) 1978
5. A. BARBU - To be published
6. P.R. OKAMOTO, A. TAYLOR and H. WIEDERSICH - "Fundamental aspects of radiation damage in Metals", eds. M.T. Robinson, F.W. Young, US-ERDA Conf. N°751006 (1975) 1188
7. G. SILVESTRE, A. SILVENT, C. REGNARD and G. SAINFORT - J. Nucl. Mat. 57 (1975) 125
8. Y. ADDA, A. BARBU, J.L. BOCQUET and G. MARTIN - Conf. Reactor Materials Science, Alushta, SSSR (1978)
9. G. MARTIN, J.L. BOCQUET, A. BARBU and Y. ADDA - Radiation effects in Breeder Reactor Structural Materials, ed. Bleiberg et al. AIME (1977) 899
10. P.P. PRONKO, P.R. OKAMOTO and H. WIEDERSICH - Proc. 3rd Int. Conf. on ion Beam Analysis (1977)
11. D.J. POTTER, L.E. REHN, P.R. OKAMOTO and H. WIEDERSICH - Scripta Met. To be published
12. P.R. OKAMOTO and H. WIEDERSICH - J. Nucl. Mat. 53 (1974) 336
13. R.A. JOHNSON and N.Q. LAM - Phys. Rev. B13 (1976) 4364; Phys. Rev. B15 (1977) 1794
14. N.Q. LAM, P.R. OKAMOTO, H. WIEDERSICH and A. TAYLOR - Met. Trans. 1978 in Press
15. G. MARTIN - Phil. Mag. (1978) in Press
16. S.I. MAYDET and K.C. RUSSELL - J. Nucl. Mat. 64 (1977) 101
17. Y. ADDA, M. BEYELER and G. BREBEC - Thin Solid Films 25 (1975) 107
18. HANSEN - Constitution of Binary Alloys - Mc Graw Hill, London (1958)
19. J.M. PELLETIER, J. MERLIN and R. BORRELLY - Met. Sci. Eng. 33 (1978) 95
20. G. LASLAZ and P. GUYOT - Acta Met. 25 (1977) 277
21. H.M. SIMPSON and R.L. CHAPLIN - Phys. Rev. 185 (1969) 958

22. O.S. OEN - ORNL Report n° 4897

23. P. VAJDA - Rev. Mod. Phys. 49 (1977) 481

24. H. HERMAN - Acta Met. 12 (1964) 765

25. S. CERESARA and F. FEDERIGHI - Phil. Mag. 9 (1964) 623

26. J.A. HORAK, T.H. BLEWITT and M.E. FINE - J. Appl. Phys. 39 (1968) 326

27. K.S. LIU, O. KAWANO, Y. MURAKAMI and H. YOSHIDA - Rad Eff. 15 (1972) 37

28. J.A. HORAK - Phil. Mag. 17 (1968) 643

29. W. SCHULE - Phil. Mag. 10 (1964) 913

30. W. SCHULE - Phil. Mag. 19 (1969) 1085

31. M. KIRITANI and N. YOSHIDA - Crystal lattice Defects 3 (1973) 83

32. M. KIRITANI and H. TAKATA - J. Nucl. Mat. 69 and 70 (1978) 277

33. S.D. HARKNESS, C.W. ALLEN and T. BLEWITT - Int. Conf. Alustha SSSR (1978)

34. D.M. MAHER and B.L. EYRE - Phil. Mag. 23 (1971) 409

35. COWLEY - Diffraction Physics, North Holland, Amsterdam (1975)

36. P.B. HIRSCH, A. HOWIE, R.B. NICHOLSON, D.W. PASHLEY and M.J. WHEELAN - Electron Microscopy of thin Crystals,Butterworths London (1967) 348

37. G. LASLAZ - Thesis (Grenoble, France) 1978

38. M. PROFANT and H. WOLLENBERGER - Phys. Stat. Sol. b71 (1975) 515

39. K. SCHROEDER and K. DETTMAN - Z. Phys. B22 (1975) 343

40. M.H. YOO and W.H. BUTLER - Phys. Stat. Sol. b77 (1976) 181

41. W.G. WOLFER and M. ASHKIN - J. Appl. Phys. 47 (1976) 791

42. W.G. WOLFER - "Fundamental aspects of radiation damage in Metals", eds. M.T. Robinson, F.W. Young, US-ERDA Conf. N°751006 (1975) 812

43. T.R. ANTHONY - Diffusion in Solids, eds.A.S.Nowick et al., Acad. Press New York (1975) 353

44. M. DOYAMA - J. Nucl. Mat. 69 and 70 (1978) 350

45. e.g. K.C. RUSSELL - Acta Met. 19 (1971) 753

46. P. BARLOW and T. LEFFERS - Phil. Mag. 36 (1977) 565

47. K.C. RUSSELL - AERE Report R. 8958 (1977)

48. K.L. BERTRAM, F.J. MINTER, J.A. HUDSON and K.C. RUSSELL - AERE Report R. 8791 (1977)

49. L. WEAVER, B. HUDSON and J. NUTTING - AERE Report R. 8850 (1977)

50. G. MARTIN - To be published

51. R.S. NELSON, J.A. HUDSON and D.J. MAZEY - J. Nucl. Mat. 44 (1972) 318

52. C.F. BILSBY - J. Nucl. Mat. 55 (1975) 125

53. A.J. ARDELL - 18th Colloque de Metallurgie - Saclay France (1975)

54. M. BARON, A. CHANG and M.L. BLEIBERG - Radiation Effects in breeder reactor structural materials, eds. Bleiberg et al. AIME, New York (1977) 395

TABLE AND FIGURE CAPTIONS

Table I : Summary of the observations

Abreviations and Symbols :

G.P. : Guinier Preston zones

P.L. : perfect dislocation loop

Zn : β phase precipitate

F.L. : Frank loop

\+ : observed

0 : not observed

* At 125°C : Experiment 18 corresponds to the lowest irradiation flux used, due to the weak defect production efficiency for the (231) orientation; 19 corresponds to a very thin sample, while 20 corresponds to a very thick one.

Table II : Evidence for a dose rate threshold for radiation induced precipitation

Gt_i : incubation dose for the occurence of clustering, or maximum total dose used when no clustering was observed

Table III : Qualitative behaviour of solute concentration fluctuations under irradiation

Fig. 1 : Imaging the β phase :

a) The HCP $(10\bar{1}0)$ and $(11\bar{2}0)$ spots as seen on the (111) f.c.c. diffraction pattern of the matrix. Some double diffraction in the HCP precipitates may be seen.

b) Dark field image of the β phase, using a $(10\bar{1}0)$ HCP spot.

c) Out of contrast image

Scale : 1 div = 50 nm.

Fig. 2 : Imaging the small clusters :

a) Dynamical two beam bright field image (g = [111]).

b) Dark field imaging using the intensity diffused in the halo around the (111) matrix spot.

c) Symmetrical multibeam contrast.

Fig. 3 : From the periphery of the electron beam towards it's center, the β phase develops at the expanse of the small clusters.

Fig. 4 : Irradiation conditions for the occurence of zinc precipitation in Al 1.9 at % Zn.

○ interstitial loops

◖ Small clusters

● β phase

□ No damage observed

--- Incoherent solvus temperature

Fig. 5 : Steady-state interstitial (i) and vacancy (v) concentration profiles (c), and fluxes (J), in a spherical cell in the presence of a sinusoïdal potential well for the interstitials $U_i = U_o (1 + \cos \pi \frac{R}{R_{cell}})$ according to equations 1 and 2. Values of the parameters used :

$G = 10^{-6}\ s^{-1}$

$K = 1.6\ 10^{8}\ s^{-1}$

$U_o/k_BT = 1.3\ 10^{-3}$

$D_i = 3.3\ 10^{-9}\ cm^2\ s^{-1}$

$D_v = 1.9\ 10^{-9}\ cm^2\ s^{-1}$

$R_{cell} = 1\ \mu m.$

For comparison, J_c represents the point defect flux towards a 40 Å radius cavity for the same value of the parameters, except for $U_o = 0$ and $C_i = C_v = 0$ at the surface of the cavity.

Fig. 6 : The cluster space.
The nodal lines are those given by eq. 8a and 8b. The arrows I and II are respectively the n and x component of the cluster velocity as predicted by 9a and b. The sign of the components of the cluster velocity is shown in each part of the cluster space. The non trivial critical point C is seen to be a saddle point.

Fig. 7 : Constructing the solute content of the critical precipitate (eq. 10a)

------ level of solute *undersaturation*

$x^{*} = (\overline{MM'})^{-3}$

TABLE I

N°	T°C	Φ 10^{19} $e^{-}cm^{-2}s^{-1}$	$\bar{G}$ 10^{-4} dpa/s	Orientation	$\bar{G}t_{Max}$ dpa	G.P.	P.L.	Zn	F.L.
1	95	14.5	88.7	(110)	47.9	+	+	+	0
2	95	4	24.4	(110)	13.2	+	+	0	0
3	95	1.52	9.17	(110)	5.0	+	+	0	0
4	115	15.8	96.4	(111)	52.0	+	+	0	0
5	135	15	91.0	(110)	40.9	+	+	+	0
6	135	15	91.0	(111)	49.1	+	+	+	0
7	135	2.5	15.0	(100)	9.63	+	+	+	0
8	150	15.7	93.6	(110)	50.5	0	0	+	+
9	150	15.3	93.0	(111)	50.2	0	0	+	+
10	150	2.2	13.4	(110)	7.24	0	0	+	+
11	185	15	91.0	(110)	44.8	0	0	+	+
12	185	16.3	99.4	(100)	46.5	0	0	+	+
13	185	2.5	15.0	(100)	4.95	0	0	+	0
14	185	2.55	15.6	(110)	2.80	0	0	+	0
15	185	0.51	3.10	(110)	0.74	0	0	0	0
16	200	14.0	85.4	(341)	61.5	0	0	+	+
17	200	1.95	11.9	(231)	12.8	0	0	0	0
18*	215	15.8	96.4	(231)	34.7	0	0	0	0
19*	215	15.2	92.7	(110)	50.0	0	0	0	+
20*	215	12.0	73.2	(110)	35.1	0	0	+	+
21	215	10.2	62.2	(111)	11.2	0	0	0	+
22	235	11.2	68.3	(112)	16.4	0	0	0	0

TABLE II

N°	T°C	Φ $10^{19} e^- cm^{-2} s^{-1}$	Gt_i dpa	Cluster observed
14	185	2.55	0.37	β + loops
15	185	0.51	0.74	-
16	200	14.0	5.12	β + loops
17	200	2.65	12.8	-

TABLE III

Solute vs defect flux	Solute cluster / point defect interaction	
	Attractive	Repulsive
↑↑	Amplification	Decay
↑↓	Decay	Amplification

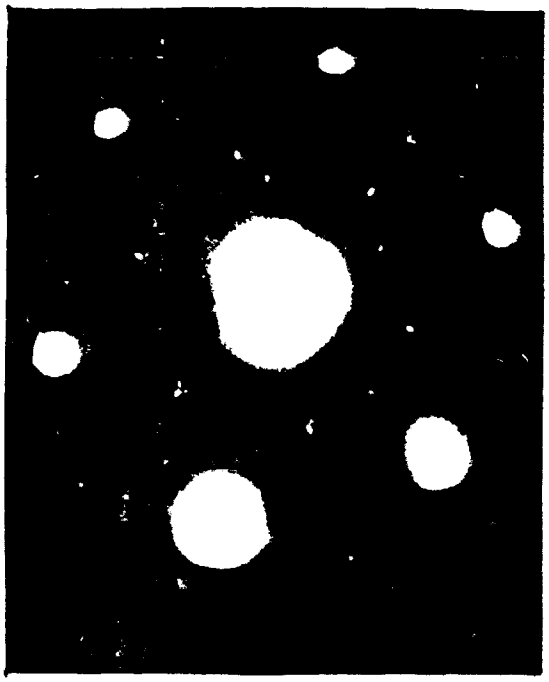

Fig 1a

1b

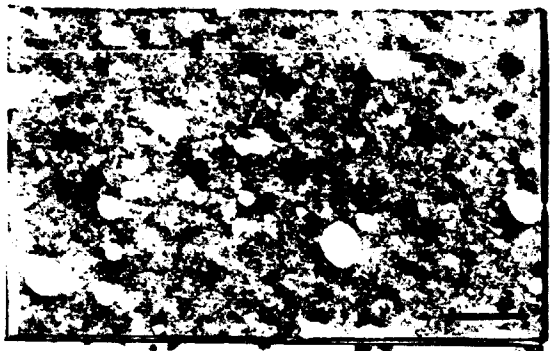

1c

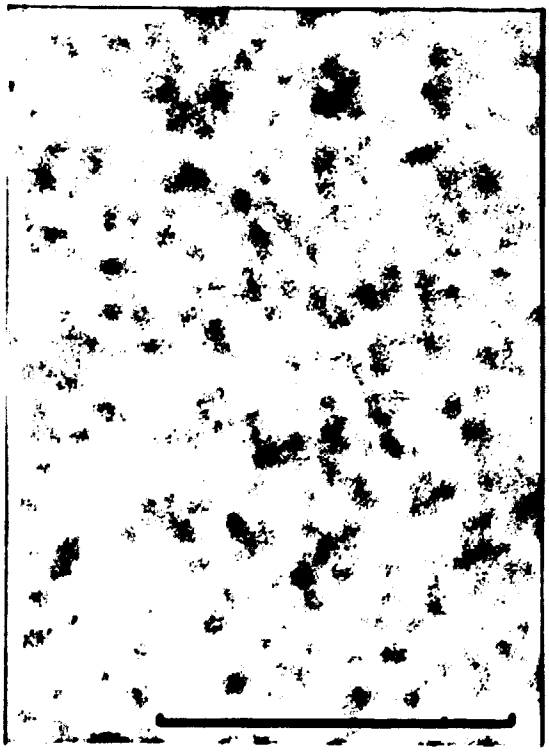

Fig 2

a

b

c

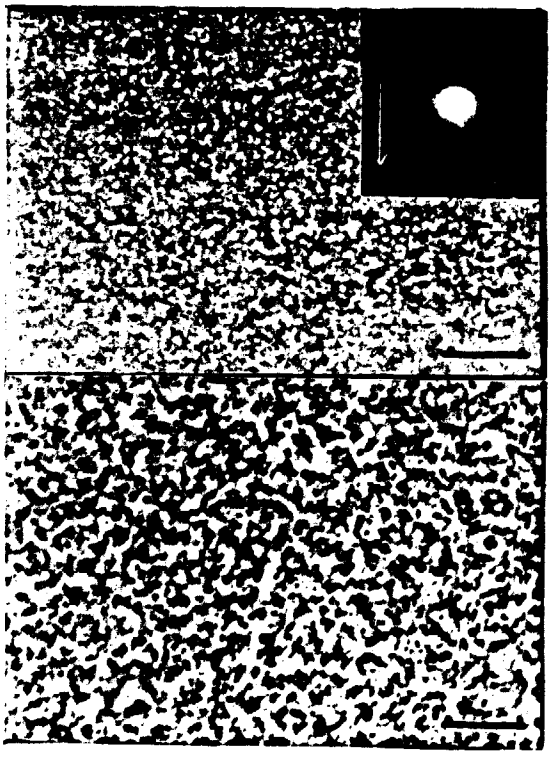

Fig 3

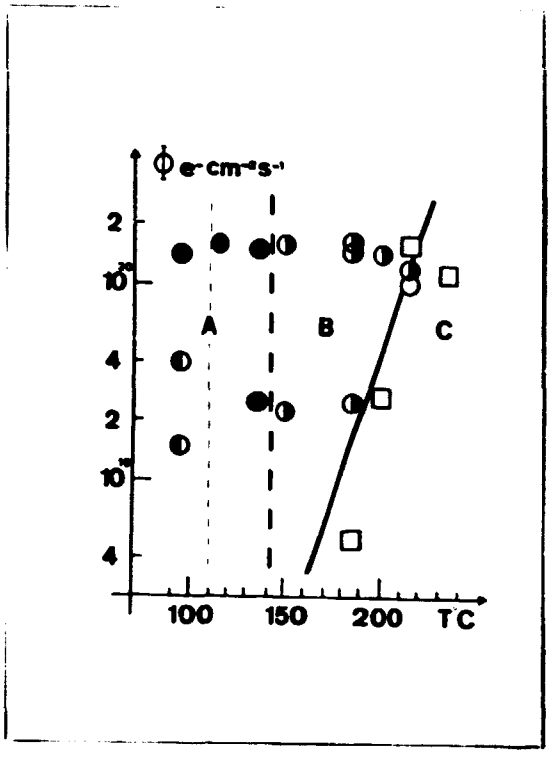
Φ e⁻ cm⁻² s⁻¹
2
10¹⁸
4
2
10¹⁷
4
A
B
C
100
150
200
TC

Fig 4

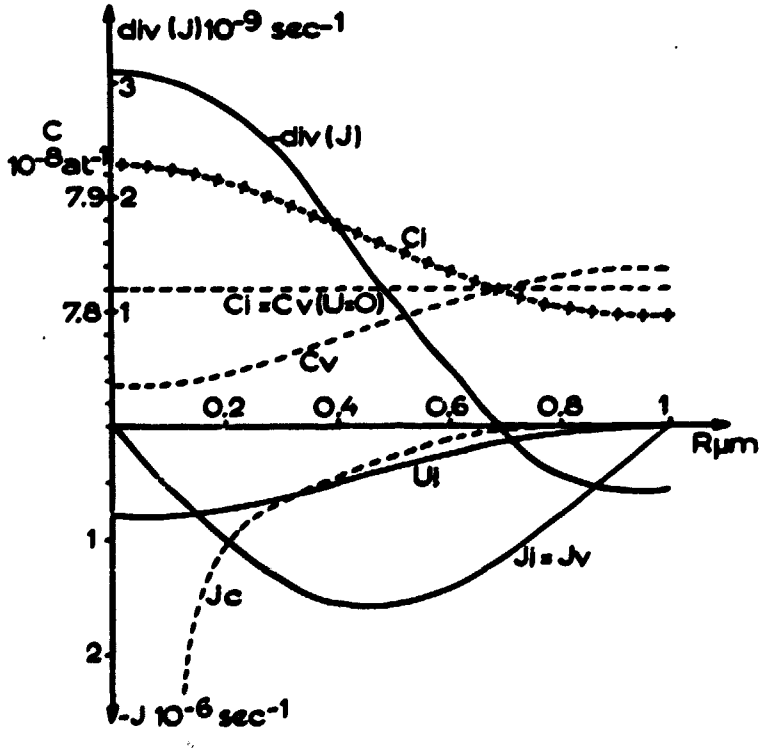
div (J) 10⁻⁹ sec⁻¹
3
C
10⁻⁸ at⁻¹
7.9
2
div (J)
Ci
7.8
1
Ci = Cv (U=0)
Cv
0.2
0.4
0.6
0.8
1
Rμm
Ui
1
Ji = Jv
Jc
2
-J 10⁻⁶ sec⁻¹

Fig 5

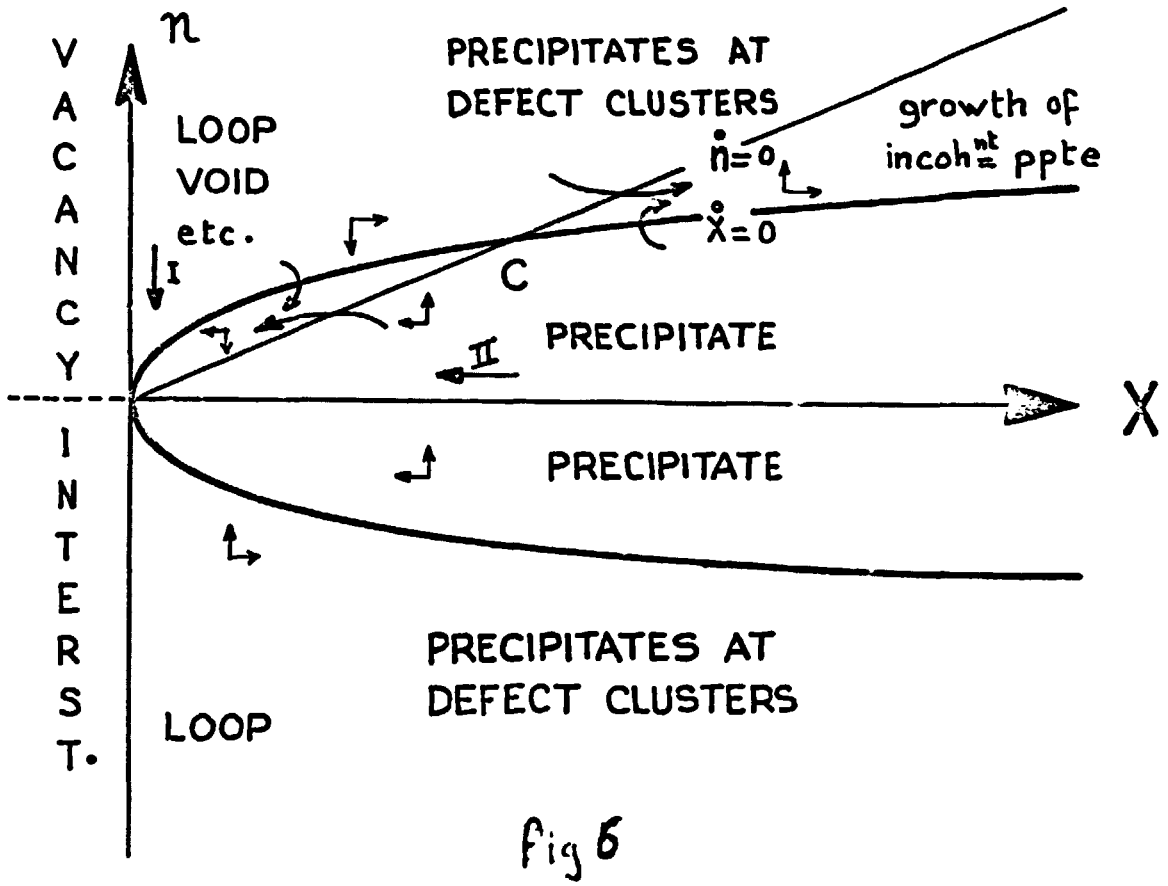
VACANCY
INTERST.
n
LOOP
VOID
etc.
LOOP
I
II
C
PRECIPITATES AT
DEFECT CLUSTERS
growth of
incoh^nt ppte
ṅ=0
Ẋ=0
PRECIPITATE
PRECIPITATE
PRECIPITATES AT
DEFECT CLUSTERS
X

Fig 6

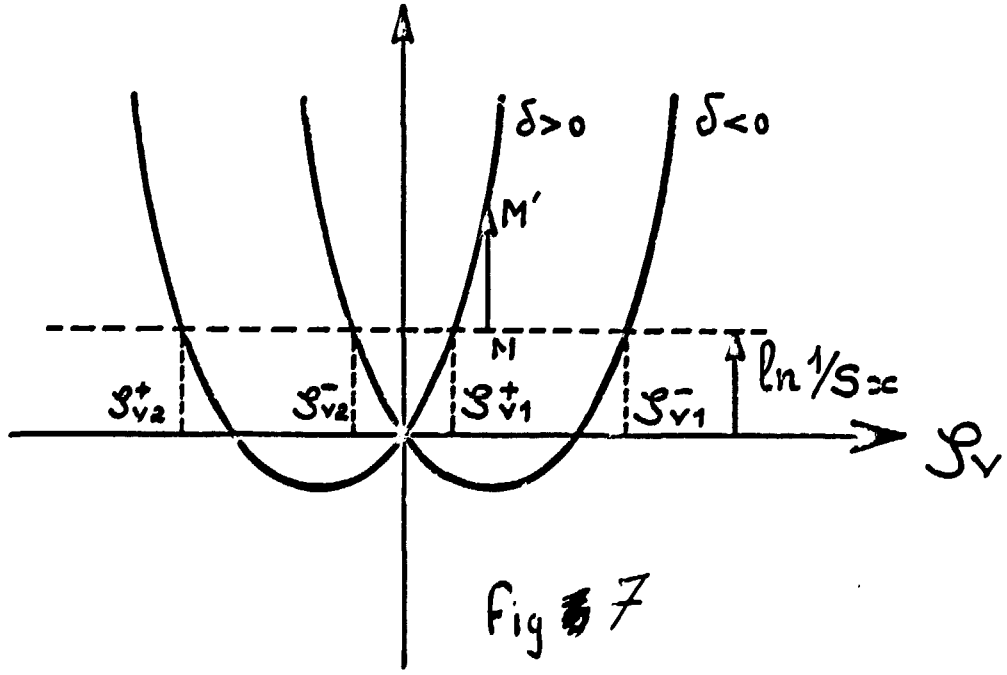
A
δ>0
δ<0
M'
M
ln 1/S∞
$\mathcal{S}_{v2}^{+}$
$\mathcal{S}_{v2}^{-}$
$\mathcal{S}_{v1}^{+}$
$\mathcal{S}_{v1}^{-}$
$\mathcal{S}_v$

Fig 7